International Journal of Research in Engineering and Science (IJRES)
ISSN (Online): 2320-9364, ISSN (Print): 2320-9356
www.ijres.org Volume 14 Issue 11 ǁ November 2026 ǁ PP. 46-56

Analysis Of Recurrent Subsidence on A National Road Segment in Watuawu Village, Lage District, Poso Regency

Yuniar Dewi[1]*, Hendra Setiawan[2], Zeffitni[3], Mohamad Sutrisno[4] , Ida Sri Oktaviana[5], Imran[6], Teguh Hilmansyah[7], Asfadi[8], Sinta. S[9]

[*1]*Department of Master's Civil Engineering, Tadulako University, Central Sulawesi, Indonesia*
[2,3,6,7,8]*Department of Civil Engineering (Morowali Regency Campus), Tadulako University, Indonesia*
[4,5]*Department of Civil Engineering, Tadulako University, Central Sulawesi, Indonesia*

Abstract
Recurrent subsidence has occurred on the national road segment at Km 233+900 in Watuawu Village, Lage District, Poso Regency, Central Sulawesi, since 2016. This study aims to identify the mechanisms and causal factors of this phenomenon. The research employed a geotechnical investigation approach and secondary data analysis, comprising the results of Standard Penetration Test (SPT), soil laboratory testing, rainfall data, seismic activity, and the morphological conditions of the Poso River. Liquefaction potential was analyzed by comparing the Cyclic Resistance Ratio (CRR) with the Cyclic Stress Ratio (CSR) to obtain the factor of safety (FS). The results show that, at depths of 2–20 m, FS values range from 0.27 to 0.55, that is, less than 1, indicating liquefaction potential in the analyzed soil layers. The recurrent subsidence appears to be associated with a combination of slope-toe erosion caused by the flow of the Poso River, increased soil saturation due to rainfall, the geotechnical conditions of the soil layers, and regional tectonic activity. This study recommends remediation through ground improvement and riverbank protection based on further geotechnical investigation. The findings are expected to serve as a basis for consideration in mitigation planning and in improving the stability of national road segments in disaster-prone regions.

Keywords: *Recurrent Subsidence, Geotechnics, Liquefaction, SPT, Road Stability.*

Date of Submission: 28-10-2026 Date of acceptance: 07-11-2026

I. INTRODUCTION

National roads, as vital connecting transportation infrastructure, must satisfy the operational standards of their service function. Failures in the soil structure that cause settlement or collapse of the ground have significant impacts on mobility, the economy, and the safety of road users (Terzaghi et al., 1997; Bowles, 2001). This condition warrants particular attention in regions composed of young alluvial sediments that remain influenced by active fluvial processes (Boggs, 2006).

Watuawu Village, located in Lage District, Poso Regency, Central Sulawesi Province, is one of the areas that is geomorphologically influenced by the presence of the Poso River. Alluvial deposits formed by sedimentation are characterized by fine-grained materials to loose, low-density sands under highly saturated conditions (Craig, 2004; Holtz et al., 2011). Soils with such properties are considered prone to excessive deformation and loss of bearing capacity, and are even at risk of liquefaction when triggered by dynamic loads or fluctuations in hydraulic conditions (Seed & Idriss, 1971; Kramer, 1996; Boulanger et al., 2014). Tectonic activity along the Poso Fault also exerts an influence.

Field observations indicate that the road in Watuawu Village has experienced recurrent subsidence events from 2016 to the present, despite the implementation of various remedial measures. The peak of the massive damage occurred on 23 January 2025, when the road suffered a major collapse. The subsided area poses a hazard to the residential settlements located around the affected site. On the basis of these field conditions, this study was conducted to identify the factors causing the recurrent subsidence of the national road in Watuawu Village by analyzing liquefaction potential and to propose remedial recommendations.

II. RESEARCH METHODOLOGY

2.1. Research Location

The study site is located precisely on the national road segment at Km 233+900, Watuawu Village, Lage District, Poso Regency, Central Sulawesi Province, at the coordinates Latitude = 1° 28' 54.66" S and Longitude =

120° 45' 51.43" E. Geomorphologically, the study site lies within an active fluvial environment influenced by the Poso River. The affected national road is characterized by the following data:

Road length : 100.0 meters
Road width : 6.0 meters
Depth : ± 3.0 meters



Figure 1. Research Location

2.2. Research Flowchart

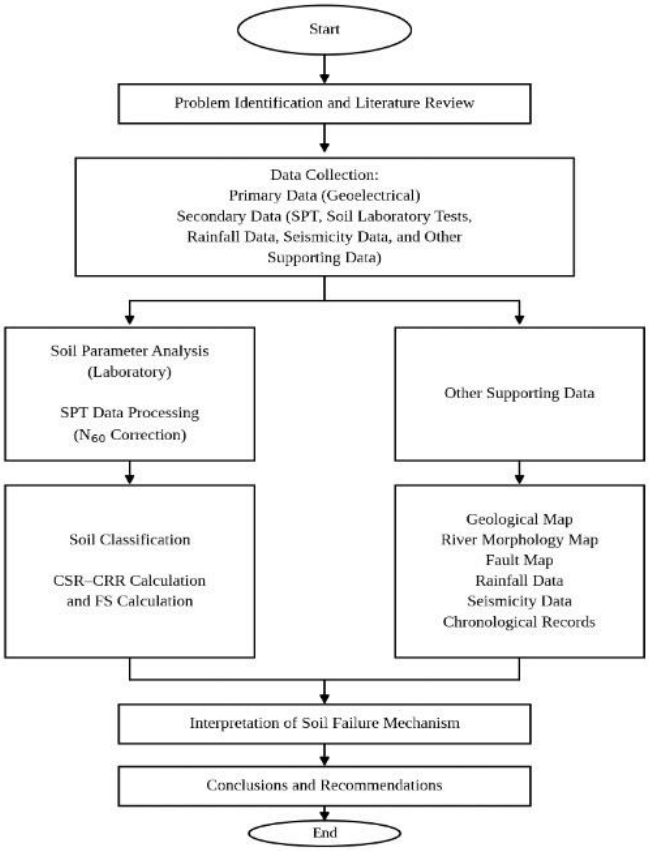


Figure 2. Research flowchart

2.3. Field Evidence Acquisition

The geotechnical investigation was conducted using core drilling results (deep boring) to validate the anomalies identified in the data. The procedure followed the method of Youd et al. (2001) and ASTM D1586, and comprised:

1. Acquisition of N-SPT values

N values were obtained at intervals of 1.5–2.0 m to map the vertical soil density profile, particularly in zones indicated to be saturated

2. Groundwater table (GWT) monitoring
   Groundwater elevation was recorded immediately after drilling and again 24 hours later to determine the static saturation level.
3. Stratigraphic identification
   Detailed documentation of the boring logs to identify the presence of fine sand layers susceptible to liquefaction

Soil samples obtained from the drilling were tested in the laboratory to determine the physical and mechanical parameters to be used in the calculation of the Liquefaction Potential Index (LPI):

1. Sieve Analysis (Grain Size Analysis)
   Determination of the percentage of fine particles (fines content) as the primary correction factor in the liquefaction resistance (CRR) analysis.
2. Atterberg Limit
   Determination of the plasticity index (PI) to evaluate the susceptibility of fine-grained soils to cyclic softening

2.4. Data Analysis Methods

Data analysis was conducted quantitatively and interpretively to evaluate geotechnical conditions, liquefaction potential, and subsurface characteristics. The analysis was based on the integration of field investigation data, laboratory test results, topographic data, river morphology, secondary seismic data, and groundwater samples from residents' wells. The stages of the data analysis methods are described as follows:

1. Liquefaction potential was analyzed using the Seed and Idriss method based on *Standard Penetration Test* (SPT) data, soil parameters obtained from laboratory testing, the groundwater table, and seismic data. The analysis stages comprised:
2. Analysis using the Seed and Boulanger method to correct the field SPT blow counts to (N1)60 values, in order to obtain a standardized value that accounts for the effects of energy, overburden pressure, and drilling conditions.
3. Calculation of the *Cyclic Stress Ratio* (CSR) as a representation of the cyclic stress induced by earthquakes, using the parameters of maximum earthquake acceleration, total stress, and effective stress of the soil.
4. Determination of the *Cyclic Resistance Ratio* (CRR) based on empirical correlations between corrected SPT values and the resistance of the soil to liquefaction.
5. Calculation of the factor of safety against liquefaction (*Factor of Safety*/FS) using the following equation:

$$FS = \frac{CRR}{CSR}$$

FS < 1 indicates that the soil layer has the potential to undergo liquefaction

In addition, a morphological analysis was conducted based on the interpretation of topographic maps, satellite imagery, existing field conditions, and river flow patterns. This analysis aims to identify the influence of the meandering pattern of the Poso River on the stability of the slope and the road body at the study site.

Groundwater analysis was conducted based on water samples collected from residents' wells with depths of less than 10 m. This analysis was used to evaluate the shallow hydrogeological conditions and the influence of soil saturation on the potential for soil deformation and liquefaction. The parameters analyzed included the groundwater table condition, turbidity, water color, sediment content, and indications of changes in water quality resulting from soil deformation activity or the movement of subsurface material

III. RESULTS AND DISCUSSION

The study site is located on the national road segment at Km 233+900 in Watuawu Village, Lage District, Poso Regency, Central Sulawesi Province. In terms of administrative layout, this area forms part of an overland transportation route that plays an important role in supporting community mobility and the distribution of goods and services to economic centers in Poso Regency and the surrounding region. Moreover, this segment belongs to the category of national roads connecting provinces and several regencies, and therefore holds a strategic role in regional connectivity and inter-regional traffic flow.



Figure 3. Study Site in Watuawu Village



Figure 4. Subsidence Point In Watuawu Village
Source : Hamdan, H. detikSulsel (2025) and BNPB (2025)

3.1. Analysis Of Geological Factors And Faults

Based on the Morphological Map of the study area (Figure 3), Watuawu Village in Lage District falls within a tectonic hill morphological zone, that is, a hilly region formed by the uplift and deformation of regional geological structures in Central Sulawesi. This is consistent with the physiographic conditions of Central Sulawesi, which are influenced by active tectonic activity and the presence of regional faults.

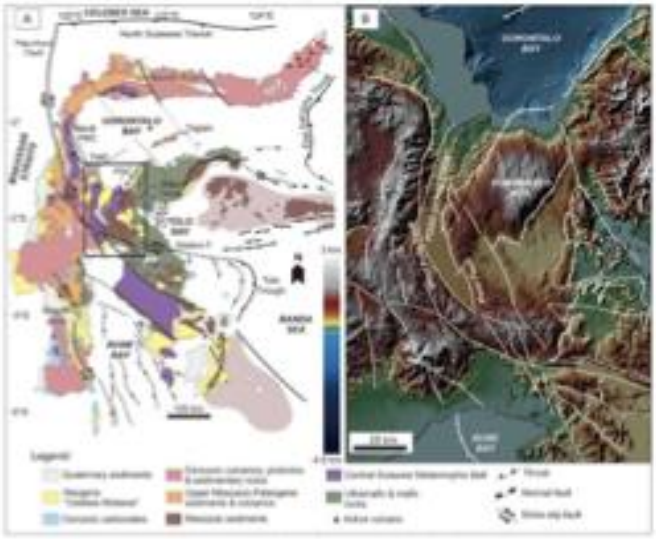


Figure 5. Morphological Map of Poso Regency
Source: Nugraha et al. (2023)

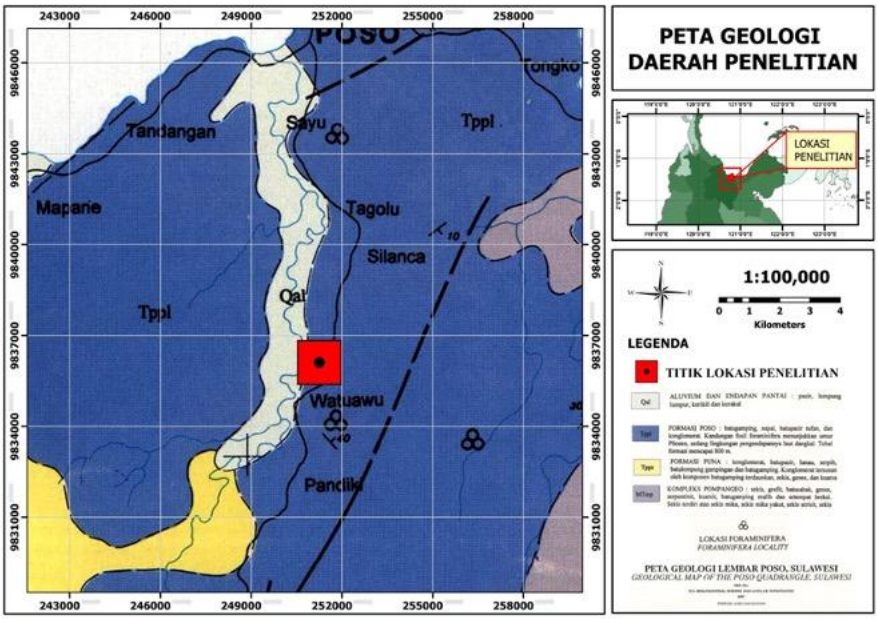


Figure 6. Geological Map of the Study Area
Source: Simandjuntak et al. (1997)

The analysis of geological factors and tectonic structures in the study area was conducted to identify the lithological types composing the bedrock and the level of structural susceptibility in Watuawu and its surroundings.

Figure 7 shows that Watuawu Village lies within the zone of influence of several active fault segments, namely the Sausu, Tokararu, Poso, and Wekuli faults.



Figure 7. Map of the *Re-plotting* Results of Active Fault Traces in the Study Area
Source: Ministry of Public Works (2024)

Based on the results of the proximity analysis (*proximity analysis*), the study area lies within the critical radius of tectonic deformation. This very short geospatial distance has significant implications from two perspectives, namely engineering (geotechnical) and landscape formation (morphological). In addition, the combination of the Poso thrust fault and the Sausu strike-slip fault near Watuawu produces complex (transpressional) tectonic forces.

3.2. Analysis Of Annual Rainfall Trends

Table 1. Characteristics and Rainfall Data

Climatic Period	Month	Rainfall Data (mm)	Rainfall Characteristics
Wet Period/Rainy Season (Rainfall > 100 mm)	March - May July - October	October 2020 : 676.5 August 2021 : 491.5 March 2025 : 379.0	High (301 – 500 mm) to very high/Extreme (Value > 500 mm)
Dry Period/Relative Dry Season (Rainfall < 60 mm)	August - October	August 2018 : 19.0 July 2018 : 23.5 October 2024 : 38.0	Low (< 100 mm)

The tabulation results indicate strong climatic variability at the study site. This phenomenon is characterized by extreme fluctuations in which the same month may be wet in one year and dry in another.
Data for the 2016–2020 period indicate a high frequency of rainfall events that may increase the risk of subsidence through intensive infiltration, which can cause sudden soil saturation and a significant increase in the soil bulk density (*bulk density*). The data also indicate a more consistent rainfall pattern, detailed as follows:

a. In 2022 and 2023, rainfall was high and evenly distributed throughout the year, which triggered a continuous risk of subsidence.
b. In 2024, the climate tended to be drier, so that the subsidence risk along the road corridor was lower.
c. In 2025, March recorded a significant increase to 379.0 mm. This surge in rainfall increased the subsidence potential again.

In general, the analysis of historical rainfall data for 2016–2025 confirms significant fluctuations in the annual precipitation index along the Poso–Tentena road corridor. This significant rainfall intensity has a high potential to influence hydrological and geotechnical conditions through three main mechanisms, namely increased infiltration of water into the soil, *surface runoff*, and sudden rises in the groundwater table. These three mechanisms contribute directly to the subsidence phenomenon at the study site.

The main impact of long-term rainfall infiltration is the periodic saturation of the soil mass. It is this degraded hydro-geotechnical condition that triggers the risk of subsidence, particularly during extreme rainy-season periods

3.3. Analysis of Regional Seismicity Characteristics

The tectonic conditions around the study site were evaluated using seismic records from the past five years. The Poso–Tentena region is influenced by the activity of local active faults that generate peak ground acceleration (PGA). Earthquake shaking acts as a dynamic load (*cyclic loading*) that imposes additional inertial forces on the riverbanks. This dynamic load is a critical triggering factor that can disturb the static stability of the slope and initiate surges of excess pore-water pressure in the saturated sandy soil layers beneath the surface.

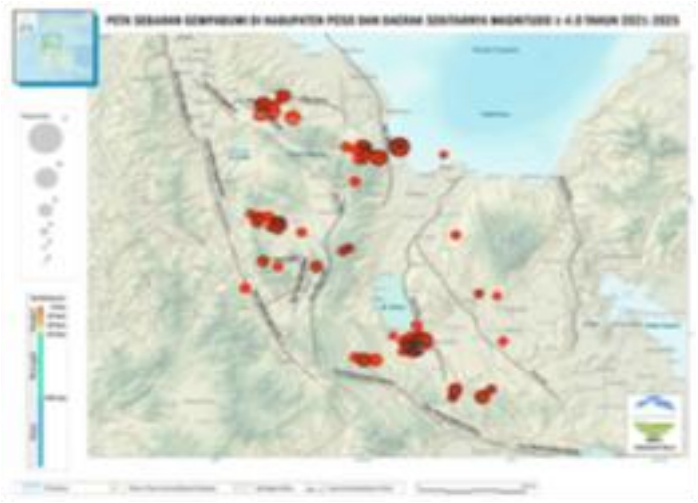


Figure 8. Distribution Map of Earthquakes in Poso Regency, 2021–2025
Source: BMKG Central Sulawesi Province (2026)

Based on the distribution map of earthquakes with M ≥ 4.0 (2021–2025), the study site is located on the Poso fault line, Tagolu–Tampemadoro segment; the epicenters are not random but form clusters that follow the

fault trend, particularly in the north, center, and south. In the north (Tagolu), earthquakes are arranged linearly, parallel to the structure, indicating an active stress-release zone. In the central part (around Lake Poso), the concentration of epicenters indicates fault segmentation or branching that intensifies deformation.

3.4. Temporal Analysis Of Cut Bank Erosion And Buffer Zone

Multi-temporal analysis based on the interpretation of aerial photographs from 2016–2025 reveals significant changes in river morphology in the study area, particularly at the bend segment of the Poso River adjacent to the road body. These changes are characterized by two main processes, namely

a. Lateral migration of the river channel (*bank migration*)
b. Bank erosion (*cut bank erosion*).

The length parameters measured in each year indicate changes in the width and position of the riverbank. These changes are directly related to the processes of lateral erosion and river channel migration (*bank migration*), which cause significant impacts on the national road and its surroundings.

Table 2. Measurement Results of *Cut Bank* and *Buffer Zone* Lengths

Year	*Cut Bank* (m)	*Buffer Zone* (m)
2016	74.08	63.08
2017	58.49	57.41
2020	59.98	50.27
2022	44.66	48.35
2023	51.58	47.74
2024	59.61	49.88
2025	48.22	56.32

The table above shows that the distance between the *cut bank* and the *buffer zone* varies from year to year. In some years the distance appears fairly large, whereas in certain years the two become closer. This condition indicates that the shape of the river bend continues to shift and change as flowing water erodes the outer side of the river, while material on the other side accumulates.

3.5. Analysis Of Geotechnical Characteristics And Liquefaction Potential



Figure 9. Location of the 2022 SPT Boring Points
Source: Soil Investigation Archive, reprocessed (2026)

3.6. Laboratory Results of Soil Parameters

In the geotechnical investigation, sampling was carried out together with *Standard Penetration Test* (SPT) testing in 2022 (secondary data) at several points around the subsidence location. These data were used to determine the soil layer sequence, relative density, and technical parameters of the subgrade. To provide a comprehensive picture of the engineering properties of the soil at the study site, the laboratory test results are presented in the following table:

Table 3. Laboratory Test Data for Point BH-01

No	Parameter and Test Description	Unit	Depth		
			4.5-5.0 m	9.5-10.0 m	14.5-15.0 m
I	***Index Properties***				
	Moisture, Density, Porosity				
1	Dry unit weight (ɣb)	g/cm³	1.45	1.36	1.43
2	Wet unit weight (ɣsat)	g/cm³	1.68	1.62	1.65
3	Natural Water Content	%	16.23	19.43	15.52
4	Specific Gravity of Soil (Gs)		2.67	2.68	2.66
5	Void Ratio		0.84	0.97	0.86
6	Porosity	%	0.46	0.49	0.46
7	Degree of Saturation	%	51.35	53.59	48.01
II	***Engineering Properties***				
	Atterberg Limits				
1	Liquid Limit (LL)		34.65	34.88	34.08
2	Plastic Limit (PL)		27.22	21.65	26.79
3	Plasticity Index (PI)		7.43	13.23	7.29
	Grain Size Analysis				
1	Retained on Sieve No. 4	%	9.42	8.42	16.84
2	Retained on Sieve No. 40	%	42.98	35.62	70.84
3	Retained on Sieve No. 200	%	78.26	69.02	91.08
4	Passing Sieve No. 200	%	21.74	30.98	8.92
5	Uniformity Coeff. (Cc)		0.29	0.25	1.61
6	Curvature Coeff. (Cu)		7.35	5.23	20.00
7	Classification (USCS)		SM	SC	SW-SM
	Direct Shear				
1	Cohesion	kg/cm²	0.024	0.025	0.017
2	Internal Friction Angle (φ)	˚	28.84	24.15	30.49
	Permeability				
1	Permeability Coefficient (k)	cm/s	4.1 x 10-5	1.7 x 10-5	1.5 x 10-3
2	Classification		Low Permeability	Low Permeability	Medium Permeability

Source: 2022 Soil Investigation Report Archive, reprocessed (2026)

The preceding table shows that the soil layers composing the study site exhibit the following characteristics:

a. Atterberg Limits
   Atterberg limit testing indicates varying consistency characteristics in the fine fraction (passing Sieve No. 40). The Liquid Limit (LL) values tend to be constant within the range of 34.08% – 34.88
b. Grain-size distribution and USCS classification
   Evaluation of the distribution using the *Unified Soil Classification System* (USCS) shows vertical changes in material facies

Table 4. Calculation of N_{60}

Depth (m)	N-SPT	C_E	C_R	N_{60}
1	0	0.92	0.75	0
2	8	0.92	0.75	6
4	11	0.92	0.85	9
6	13	0.92	0.95	11
8	14	0.92	0.95	12
10	19	0.92	1.00	17
12	22	0.92	1.00	20
14	21	0.92	1.00	19
16	26	0.92	1.00	24
18	34	0.92	1.00	31
20	38	0.92	1.00	35
22	41	0.92	1.00	38
24	44	0.92	1.00	40
26	46	0.92	1.00	42
28	57	0.92	1.00	52
30	60	0.92	1.00	55

Based on these results, the liquefaction potential analysis is presented sequentially using the laboratory test data Determination of basic input parameters
Peak ground acceleration (PGA) = 0.60 g (Poso Strong Earthquake Zone)
Design earthquake magnitude (M), M = 7.5 (Seed & Idriss method)
Groundwater table, fully saturated over the range of the affected samples (z = 4.5 – 15.0 m)
Soil density (*Bulk Density*, γ), averaged over the sample table, = 1.65 g/cm^3 = 16.5 kN/m^3

Table 5. Results of the Factor of Safety Calculation

z (m)	$CRR_{7.5}$	CSR	FS = CRR/CSR	Criterion	Remarks
2	0.103	0.384	0.27	< 1	Liquefaction
4	0.123	0.378	0.32	< 1	Liquefaction
6	0.128	0.372	0.34	< 1	Liquefaction
8	0.131	0.438	0.30	< 1	Liquefaction
10	0.172	0.486	0.35	< 1	Liquefaction
12	0.192	0.521	0.37	< 1	Liquefaction
14	0.476	0.546	0.33	< 1	Liquefaction
16	0.209	0.564	0.37	< 1	Liquefaction
18	0.319	0.575	0.55	< 1	Liquefaction
20	0.309	0.584	0.53	< 1	Liquefaction

Based on the analysis results at depths of 2–20 m, the factor of safety (FS) values range from 0.27 to 0.55. All FS values are less than 1, indicating that CRR is smaller than CSR, so that the soil layers have the potential to undergo liquefaction due to earthquakes. To determine the total *Liquefaction Potential Index* (LPI), refer to the calculation example below:

1. The Iwasaki method is computed by integrating the value of F = 1 – FS multiplied by the depth weighting function w(z) = 10 – 0.5z from the surface to a depth of 20 m.
   $LPI = \int_0^2 F \cdot (Fs) W_{(z)} d_z$
2. Determination of the layer centroid value (z)
   For the depth interval of 0–2 m, the mid-depth value (z_{mid}) is as follows:
   $z = \frac{0+2}{2} = 1$ m
3. Calculation of the risk factor (F)
   The risk factor (F) is calculated by substituting the FS value into the equation

F = 1 – FS
= 1 – 0.27
= 0.73

4. Calculation of the depth weighting function ($W_{(z)}$)
   The Iwasaki weighting function assigns a higher degree of importance to layers located closer to the ground surface. Substituting z = 1 m into the linear weighting formula yields:
   $W_{(z)}$ = 10 – 0.5(z)
   = 10 – 0.5(1)
   = 9.5
5. Layer contribution value
   The total contribution of this 2-m-thick layer (Δz = 2) to the global LPI is calculated by multiplying all of the above variables:
   Contribution = F x $W_{(z)}$ x Δz
   = 0.73 x 9.5 x 2
   = 13.87

The calculation results for the subsequent depth intervals are detailed in Table 6:

Table 6. LPI Calculation Results

Interval z (m)	z Mid (m)	FS	F = 1-FS	W(z)	Contribution
0 - 2	1	0.27	0.73	9.5	13.87
2 - 4	3	0.32	0.68	8.5	11.56
4 - 6	5	0.34	0.66	7.5	9.90
6 - 8	7	0.30	0.70	6.5	9.10
8 - 10	9	0.35	0.65	5.5	7.15
10 - 12	11	0.37	0.63	4.5	5.67
12 - 14	13	0.35	0.65	3.5	4.55
14 - 16	15	0.37	0.63	2.5	3.15
16 - 18	17	0.55	0.45	1.5	1.35
18 - 20	19	0.53	0.47	0.5	0.47
Total *Liquefaction Potential Index* (LPI)					**66.77**

The total *Liquefaction Potential Index* (LPI) of 67 falls into the category of very high liquefaction risk (*Severe*/*Very High* liquefaction if LPI > 15).

3.7. Multi-Parameter Integration Analysis of the Subsidence Phenomenon

The integration of seismic, climatological, lithological, and river morphological data reveals a unified mechanical system that controls both short-term and long-term subsidence. This complexity is initiated by a macro-scale tectonic control, namely the proximity of the site to the Poso Fault (1.60 km), which creates a subsurface *weak plane*. This weakening factor is exacerbated by the infiltration of extreme rainfall in the 10-year dataset, which triggers *water table fluctuation* driven by fluctuations in river discharge, as well as internal erosion (*piping*) resulting from the washing away of fine particles that have collapsed under daily *traffic loading*.

Concurrently, the helicoidal flow of the meandering Poso River aggressively scours the outer wall of the bend (*riverbank scouring*), reducing the *buffer zone* from 63.08 m to a critical 47.74 m and creating a lateral free face. When the soil factor of safety declines to FS < 1.0 and the foundation loses its bearing capacity because of liquefied sand, daily micro-seismic vibrations act as the final trigger, forcing the thick soil block to collapse vertically (*sinkhole effect*) while simultaneously displacing horizontally as lateral *spreading*, which threatens the stability of the national road

Based on the results of the geotechnical analysis of the *domino effect* occurring at the study site, the technical recommendations and disaster mitigation measures for remediation are as follows:

a. Cement Grouting
   Filling of voids with cement *slurry*/*foam mortar* (lightweight foamed concrete) to prevent collapse of the cavity roof (*roof collapse*) during pile driving.
b. River Bend Protection (*Cut Bank Protection*)
   Installation of continuous *secant piles* or steel *sheet piles* along the outer edge of the river bend, combined with groynes (*groyne*), to deflect the helicoidal flow of the Poso River and halt slope-toe erosion (*toe erosion*).

IV. CONCLUSIONS

Based on a geotechnical forensic approach, the recurrent subsidence phenomenon results from a cascading structural failure (*domino effect*) controlled by the following four causal factors:

a. Lateral triggering factor (meandering river morphology)
   The flow of the Poso River erodes the slope toe (*toe erosion*) and reduces the *buffer zone* from 63.08 m (2016) to a critical 47.74 m (2023), thereby eliminating the lateral restraining force of the riverbank.
b. Internal weakening factor
   The clay layer of the Tppl Formation (0 – 38 m) traps water as a result of extreme monthly rainfall of up to 676.5 mm (October 2020) and 379.0 mm (March 2025), which triggers excessive pore-water pressure.
c. Foundation instability factor (Liquefaction)
   The analysis results at depths of 2–20 m show factor of safety (FS) values ranging from 0.27 to 0.55. All FS values are less than 1, indicating that CRR is smaller than CSR, so that the soil layers have the potential to undergo liquefaction due to earthquakes, with a critical LPI index of 67 that triggers the collapse of subsurface cavities.

REFERENCES

[1]. AASHTO. (2018). Earthwork Series – Fill Placement: Unified Soil Classification System (USCS) Guide. American Association of State Highway and Transportation Officials, Washington, D.C.
[2]. Boggs, S. (2006). Principles of Sedimentology and Stratigraphy. Pearson Prentice Hall, Upper Saddle River.
[3]. Boulanger, R. W., & Idriss, I. M. (2014). CPT and SPT Based Liquefaction Triggering Procedures (Report No. UCD/CGM-14/01). Center for Geotechnical Modeling, Davis.
[4]. Bowles, J. E. (2001). Foundation Analysis and Design. Irwin/McGraw-Hill, Boston.
[5]. Craig, R. F. (2004). Craig's Soil Mechanics (7th ed.). Spon Press, London.
[6]. Holtz, R. D., Kovacs, W. D., & Sheahan, T. C. (2011). An Introduction to Geotechnical Engineering (2nd ed.). Pearson, Upper Saddle River.
[7]. Iwasaki, T., Arakawa, T., & Tokida, K. (1982). "Simplified Procedures for Assessing Soil Liquefaction during Earthquakes". Proceedings of the Soil Dynamics and Earthquake Engineering Conference, Southampton, 1982, 925–939.
[8]. Kramer, S. L. (1996). Geotechnical Earthquake Engineering. Prentice-Hall, Upper Saddle River.
[9]. Seed, H. B., & Idriss, I. M. (1971). "Simplified Procedure for Evaluating Soil Liquefaction Potential". Journal of the Soil Mechanics and Foundations Division, Vol. 97(9), 1249–1273.
[10]. Simandjuntak, T. O., Surono, & Supandjono, J. B. (1997). Peta Geologi Lembar Poso, Sulawesi Tengah. Pusat Penelitian dan Pengembangan Geologi, Bandung.
[11]. Terzaghi, K., Peck, R. B., & Mesri, G. (1997). Soil Mechanics in Engineering Practice (3rd ed.). Wiley, New York.
[12]. Youd, T. L., Idriss, I. M., et al. (2001). "Liquefaction Resistance of Soils: Summary Report from the 1996 NCEER and 1998 NCEER/NSF Workshops on Evaluation of Liquefaction Resistance of Soils". Journal of Geotechnical and Geoenvironmental Engineering, Vol. 127(10), 817–833.